LETTER

Levantine cranium from Manot Cave (Israel) foreshadows the first European modern humans

Israel Hershkovitz[1,2]*, Ofer Marder[3]*, Avner Ayalon[4], Miryam Bar-Matthews[4], Gal Yasur[4], Elisabetta Boaretto[5], Valentina Caracuta[5], Bridget Alex[5,6], Amos Frumkin[7], Mae Goder-Goldberger[8], Philipp Gunz[9], Ralph L. Holloway[10], Bruce Latimer[11,12], Ron Lavi[13], Alan Matthews[14], Viviane Slon[1]†, Daniella Bar-Yosef Mayer[2], Francesco Berna[15], Guy Bar-Oz[16], Reuven Yeshurun[16], Hila May[2,17], Mark G. Hans[12], Gerhard W. Weber[18,19] & Omry Barzilai[20]

A key event in human evolution is the expansion of modern humans of African origin across Eurasia between 60 and 40 thousand years (kyr) before present (BP), replacing all other forms of hominins[1]. Owing to the scarcity of human fossils from this period, these ancestors of all present-day non-African modern populations remain largely enigmatic. Here we describe a partial calvaria, recently discovered at Manot Cave (Western Galilee, Israel) and dated to 54.7 ± 5.5 kyr BP (arithmetic mean ± 2 standard deviations) by uranium–thorium dating, that sheds light on this crucial event. The overall shape and discrete morphological features of the Manot 1 calvaria demonstrate that this partial skull is unequivocally modern. It is similar in shape to recent African skulls as well as to European skulls from the Upper Palaeolithic period, but different from most other early anatomically modern humans in the Levant. This suggests that the Manot people could be closely related to the first modern humans who later successfully colonized Europe. Thus, the anatomical features used to support the 'assimilation model' in Europe might not have been inherited from European Neanderthals, but rather from earlier Levantine populations. Moreover, at present, Manot 1 is the only modern human specimen to provide evidence that during the Middle to Upper Palaeolithic interface, both modern humans and Neanderthals contemporaneously inhabited the southern Levant, close in time to the likely interbreeding event with Neanderthals[2,3].

Manot is an active karstic cave located 40 km northeast of the Mount Carmel cave sites (Fig. 1). Archaeological material retrieved in five excavation seasons (2010–2014) currently indicates that the cave was intensively occupied during the early Upper Palaeolithic period[4], and, to a lesser extent, during the Initial Upper Palaeolithic and late Middle Palaeolithic periods (Supplementary Information A and Extended Data Figs 1 and 2). The original cave entrance was blocked following the collapse of the roof, probably between 30 kyr and 15 kyr ago[4]. The archaeological evidence from the cave indicates two major cultural events. The first is associated with the earlier dispersal of anatomically modern humans (AMHs) (Middle Palaeolithic), best represented in the Near East by the Qafzeh and Skhul fossils (~120–90 kyr ago)[5]. The second corresponds to the colonization of the Eastern Mediterranean region by 'modern humans' ~45 kyr ago (Upper Palaeolithic), presumably replacing the Neanderthals (for example, fossils from Amud, Kebara and Dederiyeh) in the region (~65–50 kyr ago)[6].
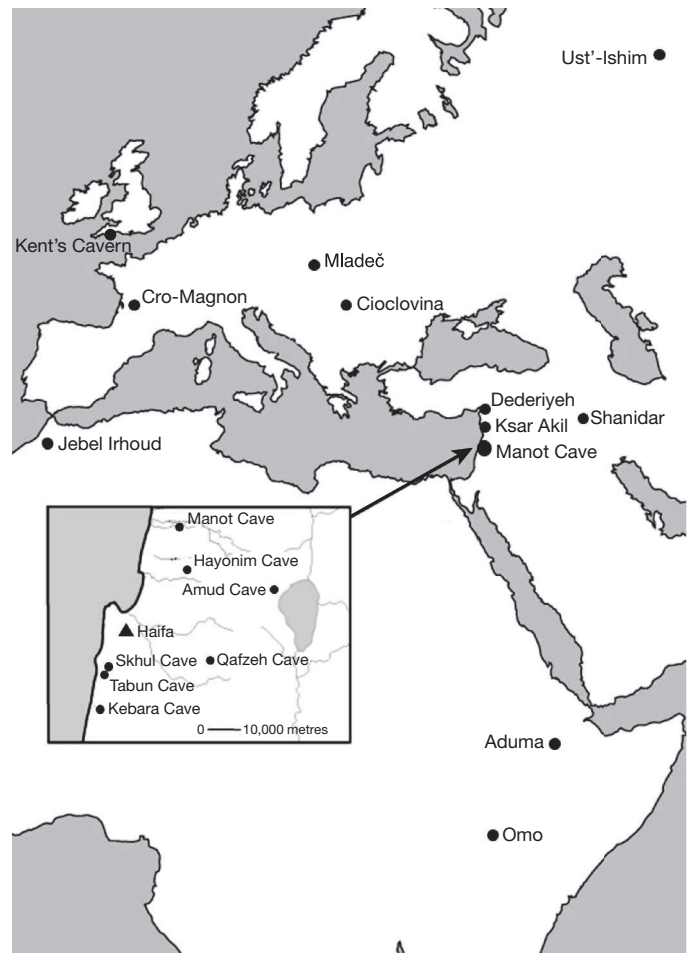

Figure 1 | Geographical location of Manot Cave, Israel. Middle Palaeolithic and Upper Palaeolithic sites with human remains are marked. Manot 1 is penecontemporaneous with the nearby Neanderthals of Amud and Kebara Caves (insert map) and older than all European Upper Palaeolithic specimens (large map). The nearby sites of Skhul, Kebara and Tabun Caves are situated on the western slope of Mount Carmel. The modern city of Haifa is shown (black triangle).

[1]The Dan David Laboratory for the Search and Study of Modern Humans, Sackler Faculty of Medicine, Tel Aviv University, PO Box 39040, Tel Aviv 6997801, Israel. [2]The Steinhardt Museum of Natural History and National Research Center, Tel Aviv University, PO Box 39040, Tel Aviv 6997801, Israel. [3]Archaeology Division, Ben-Gurion University of the Negev, PO Box 653, Beer-Sheva 8410501, Israel. [4]Geological Survey of Israel, 30 Malkhe Israel Street, Jerusalem 95501, Israel. [5]Max Planck Society-Weizmann Institute Center for Integrative Archaeology and Anthropology, D-REAMS Radiocarbon Laboratory, Weizmann Institute of Science, Rehovot 76100, Israel. [6]Department of Anthropology and Human Evolutionary Biology, Harvard University, 11 Divinity Avenue, Cambridge, Massachusetts 02138, USA. [7]Department of Geography, The Hebrew University of Jerusalem, Jerusalem 91905, Israel. [8]Institute of Archaeology, The Hebrew University of Jerusalem, Mount Scopus, Jerusalem 91905, Israel. [9]Department of Human Evolution, Max-Planck-Institute for Evolutionary Anthropology, Deutscher Platz 6, D-04103, Leipzig, Germany. [10]Department of Anthropology, Columbia University, New York 10027, USA. [11]Department of Anatomy, Case Western Reserve University, Cleveland, Ohio 44106, USA. [12]Department of Orthodontics, Case Western Reserve University School of Dental Medicine, 10900 Euclid Avenue, Cleveland, Ohio 44106, USA. [13]8 Dan Street, Modi'in 7173161, Israel. [14]Institute of Earth Sciences, The Hebrew University of Jerusalem, Edmond J. Safra Campus, Givat Ram, Jerusalem 91904, Israel. [15]Department of Archaeology, Simon Fraser University, 8888 University Drive, Burnaby, British Columbia V5A 1S6, Canada. [16]Zinman Institute of Archaeology, University of Haifa, Haifa 3498838, Israel. [17]Department of Anatomy and Anthropology, Sackler Faculty of Medicine, Tel Aviv University, PO Box 39040, Tel Aviv 6997801, Israel. [18]Department of Anthropology, University of Vienna, Althanstrasse 12–14, A-1090 Vienna, Austria. [19]The Core Facility for Micro-Computed Tomography, University of Vienna, Althanstrasse 12–14, A-1090, Vienna, Austria. [20]Israel Antiquities Authority, PO Box 586, Jerusalem 91004, Israel. †Present address: Department of Evolutionary Genetics, Max-Planck-Institute for Evolutionary Anthropology, Deutscher Platz 6, D-04103, Leipzig, Germany.
*These authors contributed equally to this work.

Table 1 | Detailed dating results of the calcitic crust covering the calvaria

Sample	^{238}U (p.p.m.)	Error	Uncorr. ^{234}U/^{238}U	Error	Corr. ^{234}U/^{238}U	Error	Uncorr. ^{230}Th/^{234}U	Error	Corr. ^{230}Th/^{234}U	Error	^{230}Th/ ^{232}Th	Error	Uncorr. age (kyr)	2σ (kyr)	Corr. age (kyr)	Error 2σ (kyr)
Inner 1	3.188	0.003	1.01712	0.00162	1.02553	0.00164	0.59892	0.00139	0.40695	0.00094	3.3	0.01	99.1	1.0	56.7	9.2
Outer 2	3.753	0.003	1.01669	0.00159	1.02131	0.00160	0.52718	0.00169	0.39903	0.00128	4.4	0.01	81.2	0.8	55.4	5.2
Inner 3	2.762	0.003	1.02060	0.00100	1.03179	0.00101	0.64550	0.00162	0.45883	0.00115	3.4	0.01	112.2	1.1	66.5	10
Outer 4	3.319	0.003	1.01540	0.00113	1.02128	0.00113	0.61236	0.00282	0.46765	0.00215	4.0	0.02	102.5	1.2	68.4	6.8
Inner 6	2.771	0.007	1.01228	0.00431	1.01598	0.00433	0.46292	0.00243	0.30355	0.00159	3.6	0.01	67.3	1.1	39.2	5.6
6+7	2.555	0.003	1.01330	0.00173	1.02000	0.00174	0.58259	0.00185	0.37654	0.00119	3.2	0.01	94.8	0.3	51.1	9.4
6+7 B after US*	1.897	0.001	1.01201	0.00201	1.01785	0.00203	0.58704	0.00300	0.38947	0.00199	3.3	0.02	96.0	1.8	53.5	9.0
8A after US	2.210	0.0015	1.02594	0.00126	1.03324	0.00127	0.45589	0.00184	0.30781	0.00124	3.9	0.02	66.0	0.7	39.9	5.2
8B after US	1.343	0.0012	1.01278	0.00190	1.02083	0.00191	0.64095	0.00603	0.41945	0.00395	3.1	0.02	110.8	3.7	59.2	11.6
9A after US	1.595	0.0013	1.01574	0.00159	1.02395	0.00160	0.60011	0.00441	0.39663	0.00291	3.2	0.03	99.5	2.4	55.0	9.6
9B after US	1.423	0.0012	1.01508	0.00152	1.02428	0.00153	0.62927	0.00507	0.40843	0.00329	3.0	0.03	107.5	3.0	57.0	11.2

Analytical errors on ages are reported as 2σ; isotopic ratios are given as 1σ. Uncorr., uncorrected; Corr., corrected; Inner and Outer, the inner and outer parts of the calvaria; after US, after ultrasonic treatment (see explanation in Supplementary Information B.2).

The Manot calvaria (Manot 1) was found on a flowstone ledge within a side chamber in the northern-most area of the cave (Supplementary Information A and Extended Data Fig. 1). A thin calcite patina mixed with detrital materials, mainly clay and oxides/hydroxides, covers both its interior and exterior surfaces. The average corrected uranium–thorium (U–Th) age was obtained from 11 samples taken from different locations throughout the calcite patina (Extended Data Fig. 3). The results indicate a minimum age of 54.7 ± 5.5 kyr ago (arithmetic mean ± 2σ); or 51.8 ± 4.5 kyr ago (weighted mean ± 2σ) (Table 1, Supplementary Information B, Supplementary Table 1, Extended Data Table 1 and Extended Data Figs 4 and 5). The numerous speleothems inside the cave indicate that the cave was continuously wet. Thus, the calcitic crust covering the calvaria probably formed close in time to the skull's original deposition in the cave, suggesting that the minimum age closely reflects the true age of the calvaria.

Manot 1 (Fig. 2a–d) comprises the uppermost part of the frontal bone (broken 3–5 cm anterior to the coronal suture; glabella and supraciliary regions are missing), two nearly complete parietal bones and the occipital bone (broken immediately inferior to the external occipital protuberance). The calvaria is relatively small and gracile in appearance, featuring thin cranial bones (Supplementary Information C). On the basis of the synostosis of the cranial sutures, Manot 1 is the skull of an adult individual. Any determination of sex is overly speculative on the basis of the existing remains. Cranial capacity is estimated to be ~1,100 ml (Supplementary Information D).

The parietal bosses are pronounced and, in superior view, they taper gradually towards the broad frontal bone (Fig. 2a). The broadest area of the skull is high on the parietal bones, the cranial surface is flattened where the parietal bones meet along the sagittal suture, and both side walls of the skull are parallel and vertically oriented (Fig. 2c). Manot 1 thus displays features typical of modern humans (Extended Data Table 2). In contrast, in lateral aspect (Fig. 2b), the coronal suture is elevated on its external surface (coronal keel). The parietals are short, and the bregmalambda chord and arc are small, falling outside the range of Upper Palaeolithic European and modern Mediterranean human populations (Extended Data Table 3).

The Manot occiput (Fig. 2b, d) has an occipital bun, a feature very frequently found both in European Neanderthals and in the majority of early Upper Palaeolithic modern humans. It also has a spherical suprainiac fossa (Supplementary Information C and Extended Data Table 2), which involves only the external table, leaving the internal table unaffected. The fossa is opposite the sagittal sinus bifurcation, similar to the condition seen in some modern humans, but contrasting to that usually encountered in Neanderthals. In shape, it resembles the fossae found in some of the North African Epipalaeolithic skulls of Afalou/Taforalt, and in the Upper Pleistocene skull from Aduma in Africa[7], but differs from some Levantine early AMHs, such as Qafzeh 6 or Skhul 9 (ref. 8), and from the transversely elongated fossa typical of Neanderthals[9]. The occipital plane convexity index is 22.3, similar to that of Neanderthals[10] and different from that of modern humans (Extended Data Table 3). The position of opisthocranion is well above inion, and the low placement of the transverse sulcus indicates a cerebellum that occupied less of the occipital squama than in recent modern humans (Supplementary Information C). In Manot 1, inion is located below endinion, whereas in Neanderthals inion is located superior to endinion, and in recent modern humans the two landmarks usually coincide[11]. Manot 1 has a well-developed superior nuchal line that extends across the occipital bone, similar to the morphology seen in some European Upper Palaeolithic specimens (for example, Cioclovina[12]), but unlike the morphology found in Neanderthals, in which this line is often only faintly expressed. Manot 1 lacks a horizontal occipital torus, a feature commonly seen in Neanderthals, and it fails to show a genuine external occipital protuberance. This latter feature is subtly expressed as a wide, triangular and irregular tuberculum. There is, however, a pronounced fossa between the nuchal lines for the insertion of the semispinalis capitis muscle, as is commonly described in Neanderthals[13] (Supplementary Information C).

Figure 2 | Various views of the Manot 1 calvaria. a, Superior view. Note the coronal keel. **b**, Lateral view. Note the occipital bunning. **c**, Frontal view. Note the vertical orientation of the lateral walls, the moderate arch of the parietals towards the sagittal suture, and the flat sagittal area. **d**, Posterior view. Note the presence of a suprainiac fossa and the pronounced superior nuchal line.

On the basis of these morphological features, Manot 1 demonstrates a mosaic of 'archaic' and modern traits (Extended Data Table 2). The taxonomic significance of this combination of features is not immediately clear, but hominins with similar combinations persist in the fossil record across sub-Saharan Africa and the Levant until, and even after, ~35 kyr ago[12,14,15].

Geometric morphometric methods[16,17] were used to place the Manot 1 fossil in the broader context of the fossil record (Supplementary Information E and Extended Data Table 4). The first two principal components of shape space (Fig. 3a, b) explain ~62% of the total shape variance. This analysis places Manot 1 within the cloud of recent and Upper Palaeolithic modern humans—namely Mladeč 1 (~35 kyr cal. (calibrated years) BP), Předmostí 3 (~30–27 kyr cal. BP), Brno 2 (~29–28 kyr cal. BP), Pavlov (~29 kyr cal. BP), and Oberkassel (~14.7–13.7 kyr cal. BP)—and remote from other fossils from the Near East, such as Shanidar 1, Skhul 5 or Qafzeh 6. A nearest neighbour analysis (Fig. 3c), based on the full Procrustes distance, links the Manot specimen with recent African skulls and with central European Upper Palaeolithic specimens, such as Mladeč 1. Whereas Qafzeh 9 plots close to Manot 1 (Fig. 3a), several other Middle Palaeolithic Levantine fossils, such as Qafzeh 6 and Skhul 5, and some European Upper Palaeolithic fossils, such as Mladeč 5 and 6, are more distant. This is possibly due to a more pronounced expression of archaic traits, marked sexual dimorphism or even the existence of two different morphs at the same site[18]. Ohalo 2 (~22.8–22.3 kyr cal. BP), discovered 50 km southeast of Manot, falls close to Upper Palaeolithic humans from central Europe and to Manot 1 (Fig. 3a), but it is not among its nearest neighbours considering the full Procrustes distance (Fig. 3b).

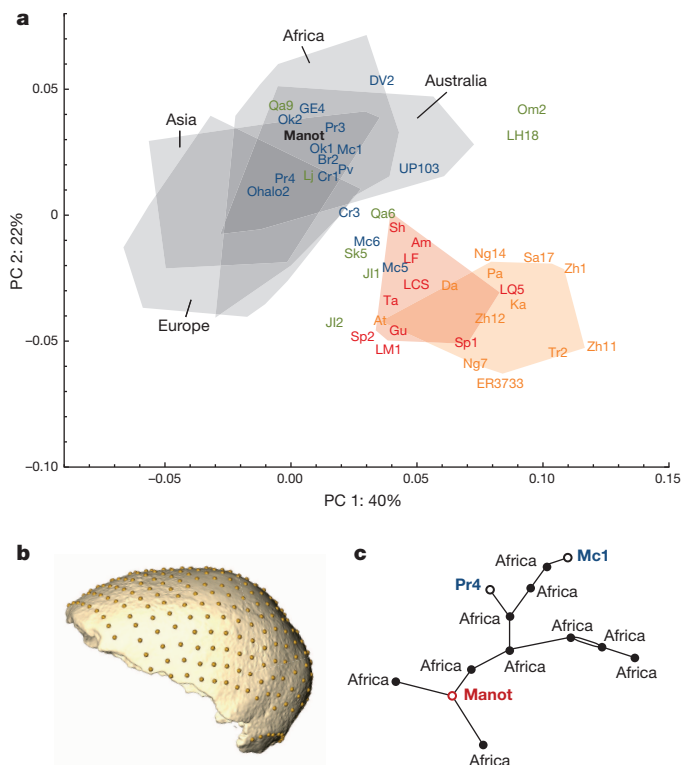The combination of discrete and metric data (Supplementary Information C) leads to our classification of the Manot 1 calvaria as a modern human. Manot 1 is thus the first direct fossil evidence that modern humans inhabited the Levantine corridor ~55 kyr ago. This period coincides with the timing predicted by genetic and archaeological models for a wave of modern human dispersal out of Africa[19–22].

The Manot 1 calvaria is similar in overall shape to early Upper Palaeolithic European skulls, and its discrete features foreshadow those of later Upper Palaeolithic humans in central Europe. This implies that the Manot people could have given rise to the first modern humans to colonize Europe successfully. Thus, the anatomical features used to support the 'assimilation model' in Europe (Neanderthal–AMH interbreeding)[8] might not have been inherited from European Neanderthals but may rather have originated from earlier Levantine populations.

The possible admixture between modern humans and Neanderthals has been extensively discussed[2,3,8,23–25] (Supplementary Information C). While perspectives based primarily on morphological information generally point to Europe as the plausible location, genetic studies suggest that interbreeding occurred in a restricted geographical area, most probably in western Asia[2,3]. Despite the differences in potential localities, most predictions focus on a period later than ~100 kyr ago[2,20], most probably between 60 kyr and 50 kyr ago[26]. The close proximity, both in terms of dates and geographical location, of Manot 1 and the Levantine Neanderthals (for example, Kebara, Amud) means that the Manot 1 specimen could potentially represent a hybrid between AMHs and Neanderthals. However, any identification of potential hybrids based solely on cranial morphology must be viewed cautiously (Supplementary Information C). An earlier interbreeding, for instance, between the Tabun Neanderthals and the Skhul AMHs who may have overlapped in time[27,28], would be in disagreement with the genetic data[3,19,20,25,26].

Manot 1 could also have been a direct descendant of early AMH populations (such as Skhul/Qafzeh), but the differences in morphology between Manot 1 and the majority of fossils from these sites render this possibility unlikely (Supplementary Information C). However, it should be noted that within- and between-group morphological variations in these populations are extremely large[18], rendering any conclusion based exclusively on morphology as tentative. Nevertheless, the absence of other AMH specimens in the Levant between the Skhul/Qafzeh material (~120–90 kyr ago) and the later appearing Manot 1 (~55 kyr ago) does not support the hypothesis of continuous representation and local evolution of AMHs in the Levant.

On the other hand, the considerably fluctuating climatic conditions during MIS 5 and 4 (favouring an alteration of differently adapted populations), the unequivocal presence of Neanderthals in the region in the time gap between early AMHs and the Manot population, and the continuing evolution of AMHs in Africa[19] advocate for the most parsimonious explanation, which is that the Manot people re-colonized the Levant from Africa, rather than evolved *in situ*.

To conclude, the Manot 1 partial calvaria represents the first fossil evidence from the critical period when genetic and archaeological models predict that African modern humans successfully migrated out of Africa and colonized Eurasia. It also represents the first fossil evidence that the Levant was occupied during the late Middle Palaeolithic not only by Neanderthals (for example, Kebara/Amud), but also by modern humans. Manot 1 provides important clues about the morphology of modern humans in close chronological proximity to a probable interbreeding event with Neanderthals[3]. Our shape analysis shows that Manot 1 is a modern human, and links its morphology to recent African skulls and to some European Upper Palaeolithic fossils. This suggests that Manot 1 probably belongs to a population that had recently migrated out of Africa and established itself in the Levantine corridor during the late Middle Palaeolithic or Middle–Upper Palaeolithic interface. This time span was favourable for human migration 'out of Africa', owing to warmer and wetter climatic events over the Northern Sahara and the Mediterranean[29]. Recent evidence points to the arrival of AMHs in Europe as early as ~45 kyr cal. BP[30]. Thus, the descendants of the Manot population could have later migrated from the Levant to Europe, establishing the early Upper Palaeolithic populations there.

Figure 3 | Comparative morphometric analysis. a, First two principal components (PC) in shape space (grey, recent modern humans of diverse geographical origins; red, Neanderthals; blue, Upper Palaeolithic modern humans; green, early *Homo sapiens*; orange, archaic hominins). **b**, Landmarks and semi-landmarks used to quantify vault shape shown on a computed tomographic scan of Manot 1. **c**, Graph of the nearest neighbours based on Procrustes distance: Manot 1 is closest to recent humans from Africa, Mladeč 1 and Předmostí 4. Abbreviations appear in Extended Data Table 4.
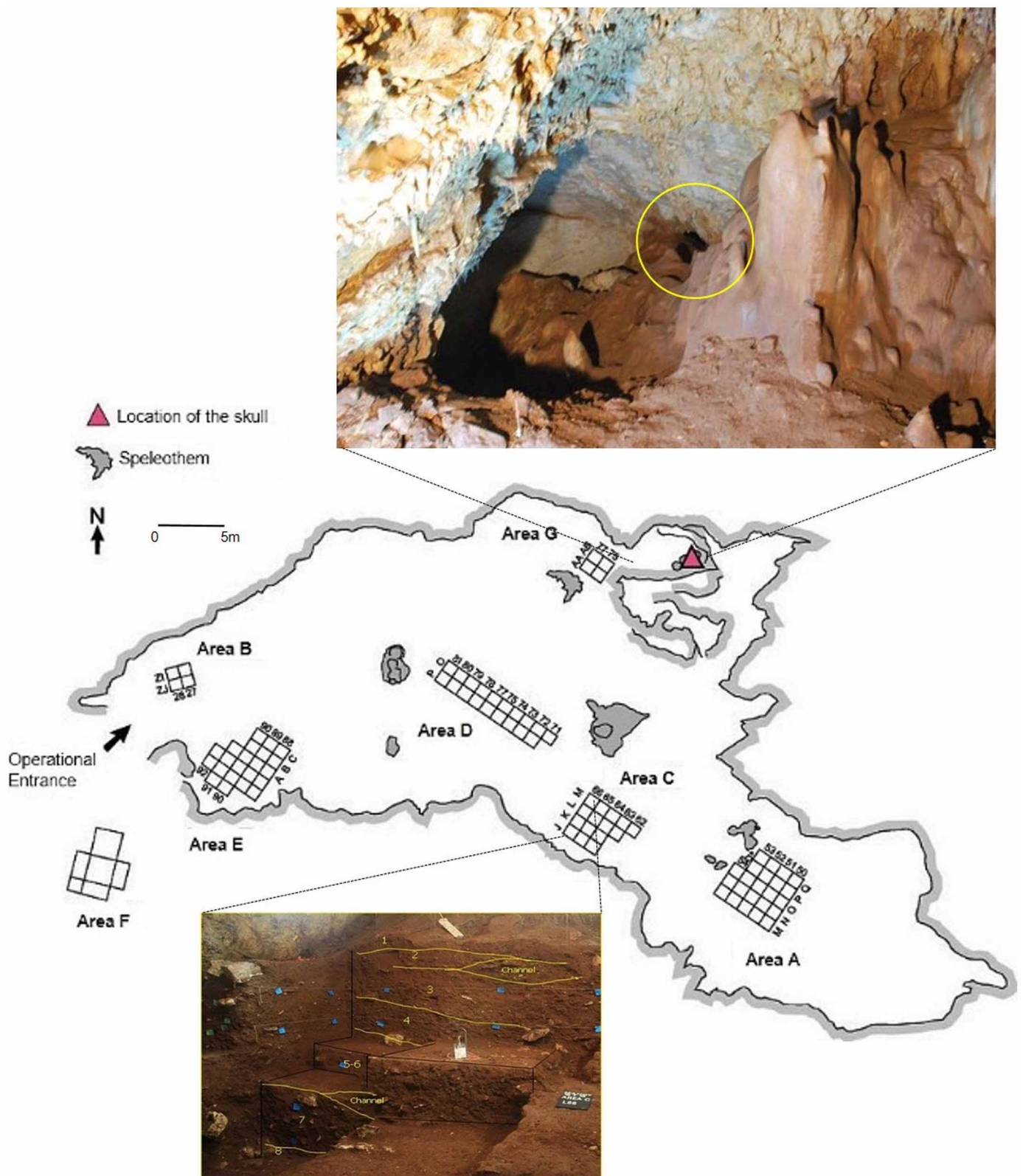
1. Hublin, J. J. The earliest modern human colonization of Europe. *Proc. Natl Acad. Sci. USA* **109,** 13471–13472 (2012).
2. Sankararaman, S., Patterson, N., Li, H., Pääbo, S. & Reich, D. The date of interbreeding between Neandertals and modern humans. *PLoS Genet.* **8,** e1002947 (2012).
3. Green, R. E. *et al.* A draft sequence of the Neandertal genome. *Science* **328,** 710–722 (2010).
4. Marder, O. *et al.* The Upper Palaeolithic Manot Cave, Western Galilee, Israel: the 2011–12 excavations. *Antiquity* **87,** http://antiquity.ac.uk/projgall/marder337 (2013).
5. Mercier, N. *et al.* Thermoluminescence date for the Mousterian burial site of Es-Skhul, Mt. Carmel. *J. Archaeol. Sci.* **20,** 169–174 (1993).
6. Valladas, H. *et al.* Thermoluminescence dates for the Neanderthal burial site at Kebara in Israel. *Nature* **330,** 159–160 (1987).
7. Haile-Selassie, Y., Asfaw, B. & White, T. D. Hominid cranial remains from Upper Pleistocene deposits at Aduma, Middle Awash, Ethiopia. *Am. J. Phys. Anthropol.* **123,** 1–10 (2004).
8. Smith, F. H., Janković, I. & Karavanić, I. The assimilation model, modern human origins in Europe, and the extinction of Neanderthals. *Quat. Int.* **137,** 7–19 (2005).
9. Balzeau, A. & Rougier, H. Is the suprainiac fossa a Neandertal autapomorphy? A complementary external and internal investigation. *J. Hum. Evol.* **58,** 1–22 (2010).
10. Hublin, J. J. in *L'Homme de Néandertal 3: l'Anatomie* 67–73 (ed. Trinkaus, E.) (E.R.A.U.L., 1988).
11. Dean, D., Hublin, J. J., Holloway, R. & Ziegler, R. On the phylogenetic position of the pre-Neandertal specimen from Reilingen, Germany. *J. Hum. Evol.* **34,** 485–508 (1998).
12. Harvati, K., Gunz, P. & Grigorescu, D. Cioclovina (Romania): affinities of an early modern European. *J. Hum. Evol.* **53,** 732–746 (2007).
13. Hublin, J. J. A propos de restes inédits du gisement de La Quina (Charente): un trait méconnu des néandertaliens et des prénéandertaliens. *Anthropologie* **84,** 81–88 (1980).
14. Crevecoeur, I., Rougier, H., Grine, F. & Froment, A. Modern human cranial diversity in the Late Pleistocene of Africa and Eurasia: evidence from Nazlet Khater, Peştera cu Oase, and Hofmeyr. *Am. J. Phys. Anthropol.* **140,** 347–358 (2009).
15. Harvati, K. *et al.* The Later Stone Age calvaria from Iwo Eleru, Nigeria: morphology and chronology. *PLoS ONE* **6,** e24024 (2011).
16. Weber, G. W. & Bookstein, F. L. *Virtual Anthropology: A Guide to a New Interdisciplinary Field* (Springer, 2011).
17. Gunz, P. *et al.* Early modern human diversity suggests subdivided population structure and a complex out-of-Africa scenario. *Proc. Natl Acad. Sci. USA* **106,** 6094–6098 (2009).
18. Schwartz, J. H. & Tattersall, I. Fossil evidence for the origin of Homo sapiens. *Am. J. Phys. Anthropol.* **143,** 94–121 (2010).
19. Soares, P. *et al.* The expansion of mtDNA haplogroup L3 within and out of Africa. *Mol. Biol. Evol.* **29,** 915–927 (2012).
20. Ingman, M., Kaessmann, H., Pääbo, S. & Gyllensten, U. Mitochondrial genome variation and the origin of modern humans. *Nature* **408,** 708–713 (2000).
21. Mellars, P., Gori, K. C., Carr, M., Soares, P. A. & Richards, M. B. Genetic and archaeological perspectives on the initial modern human colonization of southern Asia. *Proc. Natl Acad. Sci. USA* **110,** 10699–10704 (2013).
22. Reyes-Centeno, H. *et al.* Genomic and cranial phenotype data support multiple modern human dispersals from Africa and a southern route into Asia. *Proc. Natl Acad. Sci. USA* **111,** 7248–7253 (2014).
23. Wolpoff, M. H., Hawks, J., Frayer, D. W. & Hunley, K. Modern human ancestry at the peripheries: a test of the replacement theory. *Science* **291,** 293–297 (2001).
24. Duarte, C. *et al.* The early Upper Paleolithic human skeleton from the Abrigo do Lagar Velho (Portugal) and modern human emergence in Iberia. *Proc. Natl Acad. Sci. USA* **96,** 7604–7609 (1999).
25. Reich, D. *et al.* Genetic history of an archaic hominin group from Denisova Cave in Siberia. *Nature* **468,** 1053–1060 (2010).
26. Fu, Q. *et al.* Genome sequence of a 45,000-year-old modern human from western Siberia. *Nature* **514,** 445–450 (2014).
27. Grün, R. *et al.* U-series and ESR analyses of bones and teeth relating to the human burials from Skhul. *J. Hum. Evol.* **49,** 316–334 (2005).
28. Grün, R. & Stringer, C. Tabun revisited: revised ESR chronology and new ESR and U-series analyses of dental material from Tabun C1. *J. Hum. Evol.* **39,** 601–612 (2000).
29. Bar-Matthews, M., Ayalon, A., Gilmour, M., Matthews, A. & Hawkesworth, C. J. Sea-land oxygen isotopic relationships from planktonic foraminifera and speleothems in the Eastern Mediterranean region and their implication for paleorainfall during interglacial intervals. *Geochim. Cosmochim. Acta* **67,** 3181–3199 (2003).
30. Higham, T. *et al.* The timing and spatiotemporal patterning of Neanderthal disappearance. *Nature* **512,** 306–309 (2014).
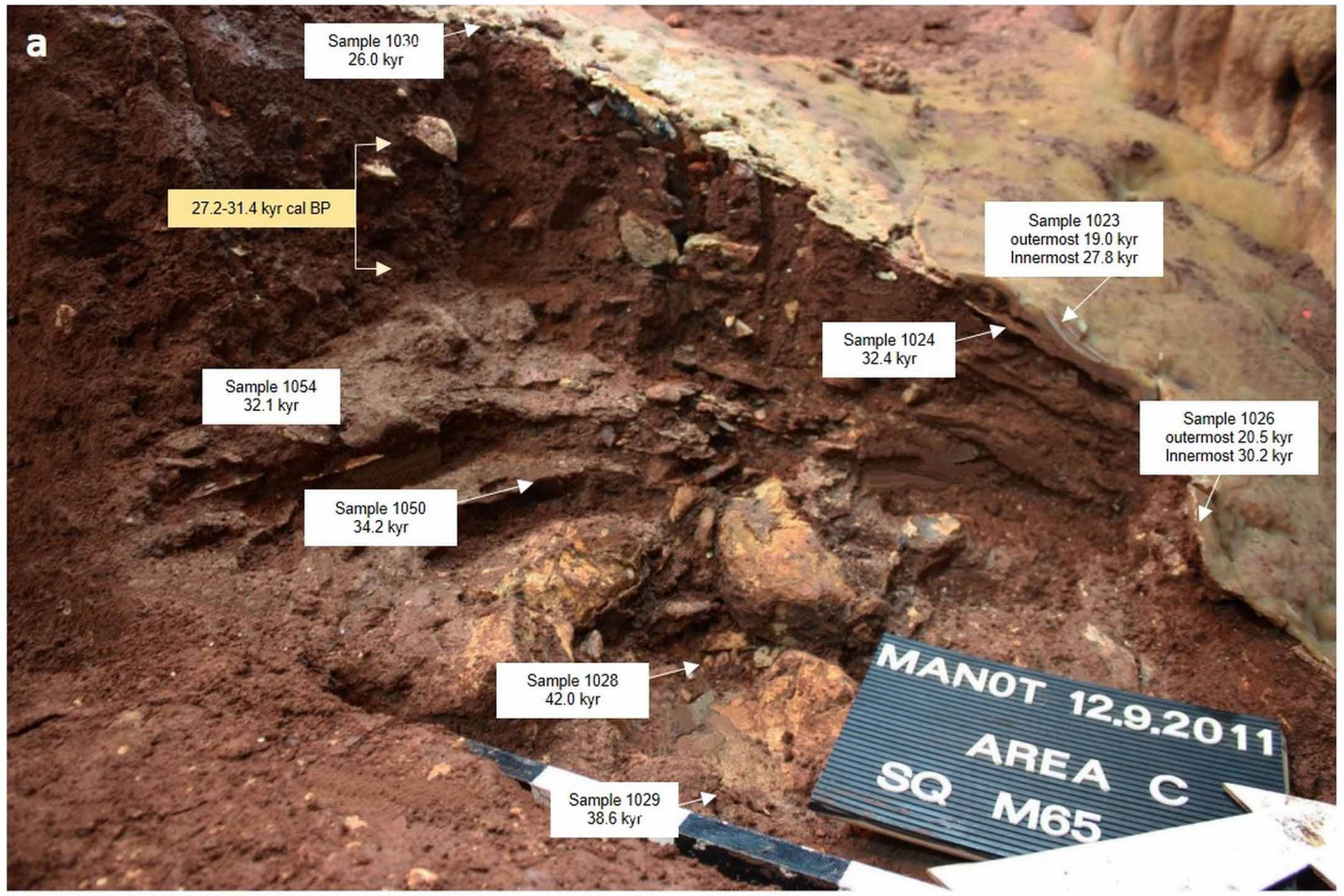
Extended Data Figure 1 | Plan of Manot Cave. The excavation areas are shown. The upper photograph shows the chamber in which Manot 1 was found (yellow circle) (looking east). The lower photograph shows the stratigraphic profile of Area C (looking west). Note the eight different sedimentological units.
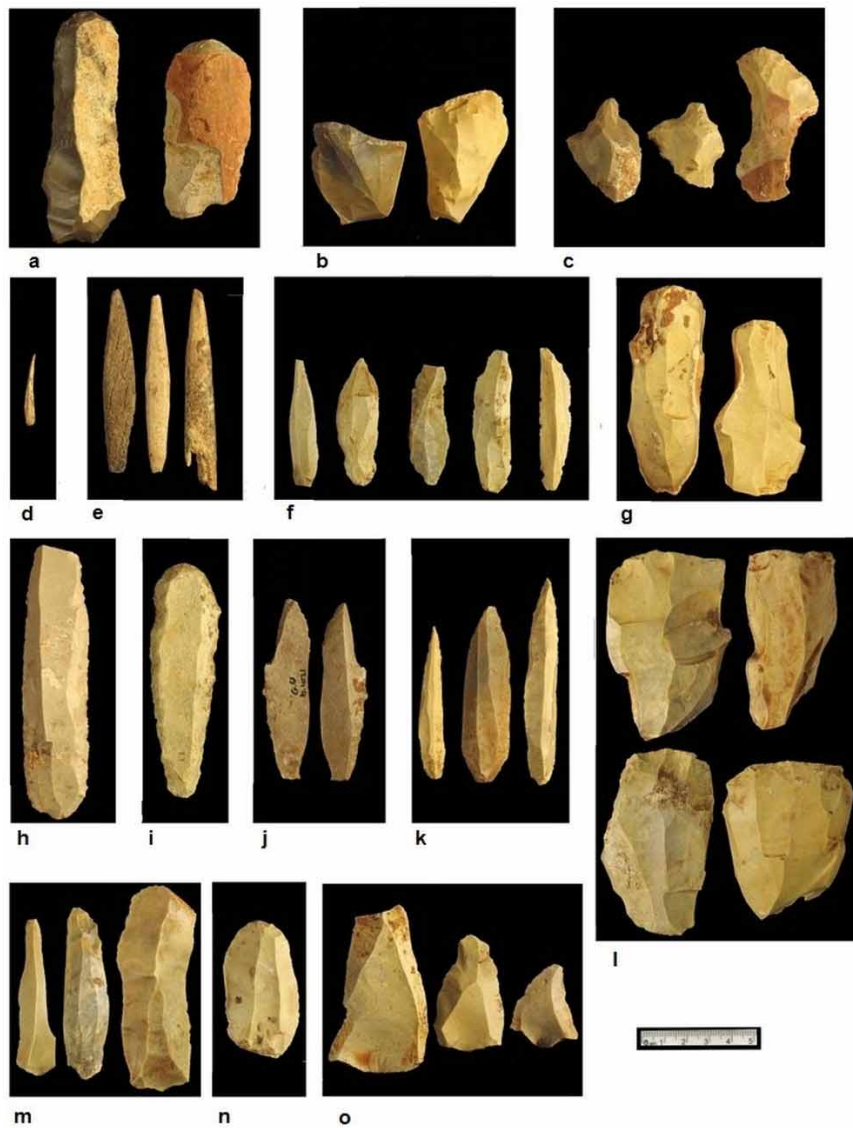
Extended Data Figure 2 | Diagnostic flint and bone artefacts from Area C. Upper Palaeolithic, **a–k**; Initial Upper Palaeolithic, **l–n**; Middle Palaeolithic, **o. a**, Aurignacian endscrapers. **b**, Carinated endscrapers. **c**, Nosed endscrapers. **d**, Curved–twisted bladelet. **e**, Antler spear points. **f**, Ahmarian blades. **g**, Ahmarian blade cores. **h**, Retouched blade. **i**, Endscraper on a blade. **j**, Burin on truncation on a blade. **k**, El-Wad points. **l**, Wide blade cores. **m**, Blades with faceted butts. **n**, Endscraper. **o**, Levallois points and flakes.

Extended Data Figure 3 | Crust sampling for dating. The outer (**a**) and inner (**b**) parts of the skull showing the locations of sampling for U–Th dating and the dating results. Ages are in thousands of years, errors are at 2σ.

Extended Data Figure 4 | Dating results for Area C. a, U–Th dates (white boxes) are of flowstone layers and the crust covering an archaeological artefact (sample 1029). Radiocarbon dates (yellow box) are of the archaeological accumulation between the flowstone layers of square M65. **b**, Dates of radiocarbon samples from Squares M65 and J65. Radiocarbon sample number, material type, ^{14}C age ± 1σ, calibrated range for 68.2% and 95.4% confidence intervals, sample identity, percentage of carbon after pre-treatment and stable carbon isotopes ratio are given. Samples from square M65 are ordered according to absolute height above sea level.
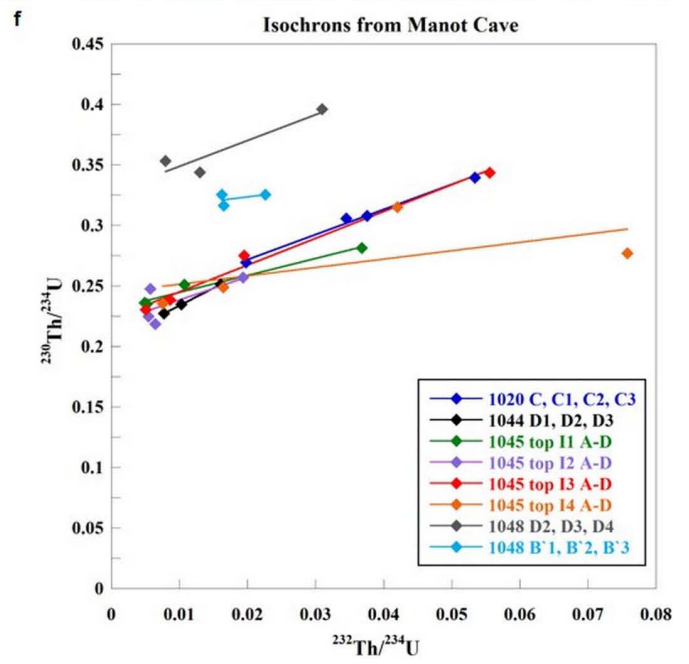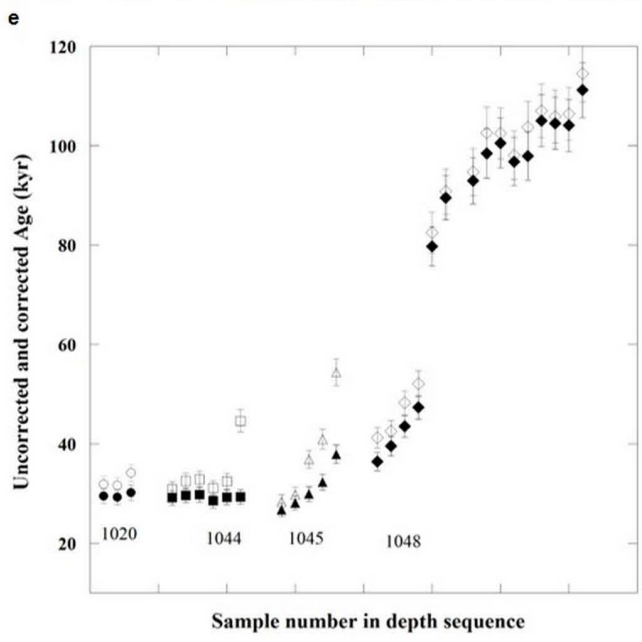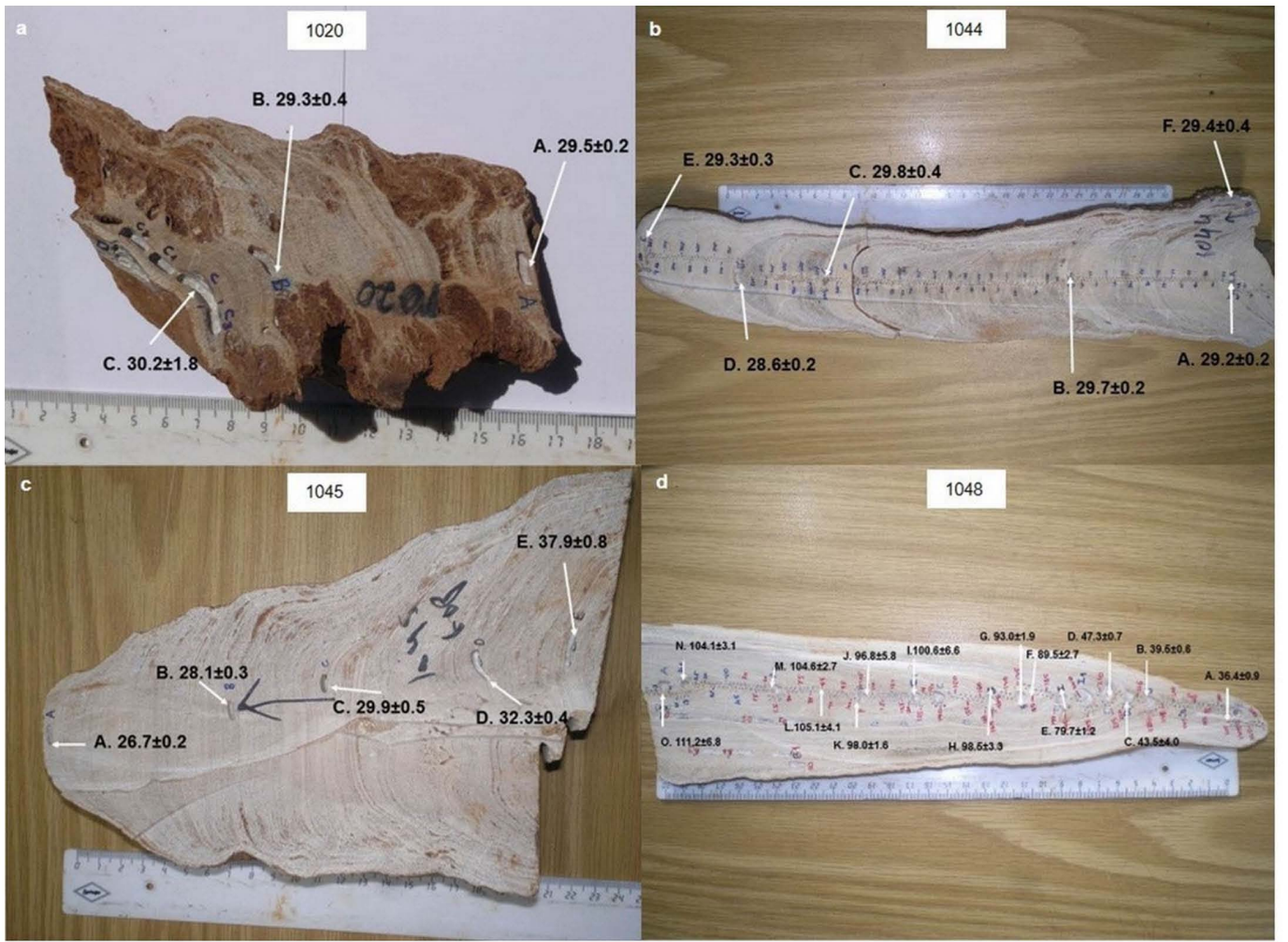
Extended Data Figure 5 | U–Th ages of stalagmites 1020, 1044, 1045 and 1048. a-d, Photographs of the stalagmites, showing the position of the dated laminae. Ages are in thousands of years, errors are at 2σ. **e**, U–Th ages of the four stalagmites, plotted in stratigraphic sequence (open symbols, uncorrected ages; solid symbols, corrected ages). Grey and black bars indicate errors on uncorrected and corrected ages, respectively. **f**, ^{230}Th/^{234}U versus ^{232}Th/^{234}U isochron plots from eight different laminae, sampled from the four speleothems.

Extended Data Table 1 | Correction factors

	Sample number				Correction factor
Isochron	1020 C,C1,C2,C3				1.14
	1044 D1,D2,D3				0.84
	1045 I1 A,B,C,D				1.67
	1045 I2 A,B,C,D				1.24
	1045 I3 A,B,C,D				1.07
	1045 I4 A,B,C,D				3.34
	1048 D2,D3,D4				0.96
	1048 B'1,B'2,B'3				3.05
	average				**1.66± 0.35**
Age correction based on comparison with a non-corrected age from the same lamina	1023-A				1.74
	1031-C				1.74
	1044-D				1.45
	1044-D3				1.73
	1045-top-I1A				2.00
	1045-top-I1C				2.20
	1045-top-I1D				1.80
	1045-top-I2D				1.30
	1045-top-I3A				1.20
	1045-top-I3B				1.10
	1045 TOP-I3C				2.80
	1045 TOP-I4A				1.30
	1045-TOP-I4D				2.90
	1048-D4				1.60
	average				**1.78±0.15**
Wiggle matching		Age uncorrected [kyr]	Age corrected [kyr]	Wiggle matching age [kyr]	
	1048-A	41.3	36.4 ±0.9	37.4	2.2
	1048-C	48.3	43.5 ±4.0	46.0	3.6
	1048-D	52.1	47.3 ±0.7	48.7	2.4
	1048-H	102.6	98.5 ±3.3	96.0	0.5
	1048-I	102.5	100.6 ±6.0	96.7	0.6
	1048-K	103.8	97.9 ±1.6	97.5	1.6
	average				**1.82±0.48**

Age correction factors and the average correction factor obtained using three methods: isochrons, correction based on comparison with non-corrected ages, and wiggle-matching.

Extended Data Table 2 | Manot 1 calvaria morphology compared with an Upper Palaeolithic European specimen, Neanderthals and present-day humans

Trait	Manot 1	Mladeč 1	Neanderthals	Recent Humans
Broadest region of skull*	High on parietal, Posterior area	High on parietal, Posterior area	Low on parietal, Posterior area	High on parietal, Posterior area
Top region of calvaria	Flatter	Well rounded	Flatter	Well rounded
Parietal convexity	Shallow	Shallow	Shallow	Marked
Side wall of calvaria	Vertical	Vertical	Rounded	Vertical
Coronal suture area	Ridge	Smooth	Smooth	Smooth
Occipital bun	Present	Present	Present	Usually absent
Suprainiac fossa	Present (Rounded shape)	Absent	Present (Transverse oval shape)	Rarely present (Rounded shape) [†]
Occipital plane convexity[‡]	Marked	Marked	Marked	Shallow
Inion location	Below endinion	Below endinion	Above endinion	Varying between below and above [§]
Transverse sulcus[‖]	Cross the parietal	Cross the parietal	Cross the occipital	Cross the parietal
Superior nuchal line	Well developed	Faintly present	Variable	Variable

* The broadest region in the Manot 1 calvaria is more forward than in Mladeč 1.
† Following ref. 9.
‡ Following ref. 10.
§ Following ref. 31.
‖ In Manot 1 the most lateral part of the transverse sulcus passes through the postero-inferior angles of the parietal bone, similarly to modern humans but unlike Neanderthals and archaic humans.

31. Balzeau, A., Grimaud-Hervé, D. & Gilissen, E. Where are inion and endinion? Variations of the exo- and endocranial morphology of the occipital bone during hominin evolution. *J. Hum. Evol.* **61,** 488–502 (2011).

Extended Data Table 3 | Manot 1 calvaria measurements compared with other archaic and modern human groups

Measurement Mean ± SD (n)	Manot 1*	Mladeč 1*	Jebel Irhoud 1†	European Neanderthals†,‡	Near East Neanderthals (Tabun, Amud, Shanidar)†	Near East AMHs (Skhul, Qafzeh)†,*	Near East Late Upper Palaeolithic (Ohalo 2)§	Near East Epipalaeolithic||	Near East Modern||
Max. Breadth (mm)	135	142	149.5	149.3±8.0 (5)	141 (Tb-1) 154 (Am-1) 154 (Sh-1)	143 (Sk-5) 145 (Sk-9) 140 (Qa-9)	144.0	M=137.1±6.3 (15) F=138.9±6.5 (8)	M=135.2±6.0 (67) F=132.5±4.7 (37)
Breg-Lambd arc (mm)	118	124	122	117.2±5.2 (5)	117 (Tb-1) 122 (Am-1) 131 (Sh-1)	131 (Sk-5) 120 (Sk-9) 145 (Qa-9)	126.0	M=137.4±5.0 (11) F=126.0±7.1 (16)	M=130.5±9.7 (68) F=128.1±9.0 (40)
Breg-Lambd chord (mm)	105	116	117	109.3±4.8 (5)	105 (Tb-1) 111 (Am-1) 118 (Sh-1)	120 (Sk-5) 112 (Sk-9) 129 (Qa-9)	116.0	M=124.6±3.9 (7) F=114.0±7.5 (4)	M=115.9±7.6 (68) F=114.1±7.5 (41)
Parietal convexity angle (degree)	140^0	143.7^0	150^0	141.8^0±5.4^0 (5)	144.4^0 (Am-1)¶	136.6^0±1.7^0 (3)	-	-	135.5^0±5.5^0 (10) M+F
Biasterion breadth (mm)	95	112	121	119.9±5.9 (5)	120 (Tb-1) 143 (Am-1) 118 (Sh-1)	122 (Sk-5) 120 (Sk-9) 111 (Qa-9)	107.0	M= 109.0±6.0 (3)	M= 106.9±4.8 (60) F=102.3±4.4 (33)
Occipital plane convexity (index)#	22.3	24.5	14.3☆	22.8±3.2 (9)**	21.1 (Am-1)¶	13.6 (Qa-9)	15.5	-	16.7±1.7 (10) †† M+F
Bone thickness at Bregma (mm)	6.0	7.0	7.6☆	6.7±1.4 (13)‡‡	9.0 (Am-1)¶	-	4.8	7.0±1.5 (10) M+F	6.4±1.7 (13) M+F

* Data from authors.
† Ref. 11.
‡ Including La Chapelle-aux-Saints, La Quina 5, La Ferrassie 1, Spy 1, Spy 2.
§ Ref. 32.
|| Ref. 33 and data from authors.
¶ Ref. 34.
#Occipital plane convexity (index) was measured as the length of the perpendicular projection (subtense) from the lambda–inion chord multiplied by 100, divided by lamdba–inion chord length.
☆ J. J. Hublin, personal communication.
** Ref. 10.
†† Ref. 10 measured a mean of 12.7 ± 3.5 for modern populations.
‡‡ Ref. 35. M, male; F, female; Sk, Skhul; Qa, Qafzeh; Tb, Tabun, Am, Amud.

32. Hershkovitz, I. *et al.* Ohalo II H2: A 19,000-year-old skeleton from a water-logged site at the Sea of Galilee, Israel. *Am. J. Phys. Anthropol.* **96,** 215–234 (1995).
33. Arensburg, B. *The People in the Land of Israel from the Epipaleolithic to the Present Times: A Study Based on their Skeleton Remains.* PhD thesis, Tel Aviv Univ. (1973).
34. Takai, H. & Suzuki, F. *The Amud Man and his Cave Site* 123–206 (Univ. Tokyo, 1970).
35. Lieberman, D. E. How and why humans grow thin skulls: experimental evidence for systemic cortical robusticity. *Am. J. Phys. Anthropol.* **101,** 217–236 (1996).

Extended Data Table 4 | Comparative data for the geometric morphometric analysis

Neanderthals (10)		Archaic *Homo* (12)	
Am	Amud 1	At*	Atapuerca SH 5
Gu	Guattari	Da	Dali
LCS	La Chapelle-aux-Saints	ER3733	KNM-ER 3733
LF	La Ferrassie 1	Ka*	Kabwe
LM	Le Moustier 1	Ng14	Ngandong 14
LQ5	La Quina H5	Ng7	Ngandong 7
Sh	Shanidar 1	Pa*	Petralona
Sp1	Spy 1	Sa17	Sangiran 17
Sp2	Spy 2	Tr2	Trinil 2
Ta	Tabun 1	Zh1	Zhoukoudian 1
Upper Palaeolithic Humans (15)		Zh11	Zhoukoudian 11
Br2	Brno 2	Zh12	Zhoukoudian 12
Cr1	Cro-Magnon 1	**Early *Homo sapiens* (8)**	
Cr3	Cro-Magnon 3	JI1	Jebel Irhoud 1
DV2	Dolní Věstonice 2	JI2	Jebel Irhoud 2
GE4	Grotte des Enfants 4	LH18*	LH 18
Mc1*	Mladeč 1	Lj	Liujiang
Mc5	Mladeč 5	Om2*	Omo 2
Mc6	Mladeč 6	Qa6	Qafzeh 6
Ohalo2	Ohalo 2	Qa9	Qafzeh 9
Ok1	Oberkassel 1	Sk5*	Skhul 5
Ok2	Oberkassel 2	**Recent Modern Humans (150)**	
Pr3	Předmostí 3	Africa	N=41
Pr4	Předmostí 4	America	N=3
Pv	Pavlov 1	Asia	N=14
UP103	Zhoukoudian Upper Cave 103	Australia	N=5
		Europe	N=85
		Papua New Guinea	N=2

The specimen abbreviations in the second column are used in the principal component analysis scores plot in Fig. 3.
* Coordinate measurements were taken on computed tomographic scans of the original.